Solid State Communications 152 (2012) 1619–1624

Contents lists available at SciVerse ScienceDirect

Solid State Communications

journal homepage: www.elsevier.com/locate/ssc

Ab initio simulation of p-type silicon crystals

E.R.L. Loustau [a,b,*], J.A. del Río [a,b], J. Tagüeña-Martínez [a], L.E. Sansores [c], R. Nava [a], M.B. de la Mora [d]

[a] Centro de Investigación en Energía, Universidad Nacional Autónoma de México (UNAM), A. P.34, CP.62580 Temixco, Morelos, Mexico
[b] Centro de Ciencias de la Complejidad (UNAM), A. P.70472, CP.04510, D.F., Mexico
[c] Instituto de Investigaciones en Materiales (UNAM), A. P.72, CP.04510 D.F., Mexico
[d] Instituto de Física (UNAM), A. P.20364, CP.04510, México D.F., Mexico

ARTICLE INFO

Article history:
Received 6 August 2011
Received in revised form
27 December 2011
Accepted 23 April 2012
by S. Scandolo
Available online 11 May 2012

Keywords:
A. Nanomaterials
A. Porous silicon
A. P-type silicon
E. Ab *initio* simulation

ABSTRACT

Porous silicon ($p-Si$) morphology depends on several parameters of the crystalline silicon substrate such as doping type and carriers concentration. Experimental results on ($p-Si$) show that although in the porous samples carriers are greatly reduced, boron atoms remain in the bulk. The study of p-type silicon crystals substrates by means of *ab initio* computational simulations will help to understand how boron atoms behave during the electrochemical reaction of porous silicon ($p-Si$) fabrication. Here we studied the properties of p-types crystalline silicon models analyzed using the ABINIT code. We constructed 4 silicon crystal models with a maximum of 216 atoms by simulation cell. The optimized geometries and some electronic properties were obtained. We observed that around the boron impurity the crystal lattice is deformed because of the bonding length **Si**–**B**. The total energy increases with the number of boron atoms by simulation cell. The relative electronic densities indicated that the charge contributions to the dangling bond, produced by the presence of the boron impurity, are mainly distributed around its first silicon neighbors.

1. Introduction

Since the discovery of porous silicon ($p-Si$) photoluminescence made by Cahnam in 1990 [1], there have been many studies focused in relating its photoluminescence spectra with the size, form and chemical species on the surface of its pores [2]. Its topological properties depend on the experimental parameters used during its fabrication [3] particularly on the doping of the crystalline sample. It is well understood that holes in the substrate are required for the *HF* chemical attack during the $p-Si$ fabrication. Therefore, it is important to study p-type silicon crystal (CSi:B) looking for regions that could promote the pores formation. Also, it is interesting to understand how and where the boron atoms remain in the $p-Si$ structure, as it has been reported [4].

We have extensively studied porous silicon, both theoretically [5–7] and experimentally [8,9]. We have successfully implemented different applications such as biosensors [10], luminescent structures [11], one dimensional photonic crystals [9], mirrors for solar concentration devices [12] and filters [9]. These diverse applications are possible varying the structure of porous silicon by changing the substrate and the electrochemical etching conditions. A crucial characteristic to take into account in the electrochemical etching is the resistivity, which is inversely proportional to the p doping level. A clear example is the fact that if we use a lightly doped silicon substrate luminescent structures are obtained, but not photonic structures, while if we use a heavily doped substrate one dimensional photonic crystals [13] which are not luminescent are built. When we try to combine the luminescent and the photonic properties in a single structure many difficulties appear [13]. Fig. 1 shows SEM images of two multilayer structures made using identical electrochemical conditions except the resistivity of the p-type silicon wafer. Clearly, there are two different topologies: at low resistivity the desired photonic structure is obtained while at high resistivity the interfaces are highly deformed.

It is known that the surface of commercial p-type silicon wafers could be irregular, and that the *HF* electrochemical attack begins at these irregularities due to a tip type effect [14]. Then, the porous formation continues due to the presence of holes. The question is, what happens to the boron atoms? Do they remain in the surface of the pore? Are they removed? Could they determine the form and the size of the porous silicon pores? In order to understand how the resistivity of the wafer determines the final porous silicon structures, we need a deeper theoretical study. Here, we present an *ab initio* computational study of p-type crystalline samples as close as possible to our experimental conditions.

The study of boron impurities (**B**) in the silicon (**Si**) lattice is not a new subject. Experimental results on this topic have been reported since the eighties; however, computational simulations of p-type silicon publications are scarce. In ref. [15] the densities

* Corresponding author at: Centro de Investigación en Energía, Universidad Nacional Autónoma de México (UNAM), A. P.34, CP.62580 Temixco, Morelos, Mexico.
E-mail addresses: emiloustau@gmail.com, erll@cie.unam.mx (E.R.L. Loustau).

0038-1098/$ - see front matter © 2012 Elsevier Ltd. All rights reserved.
http://dx.doi.org/10.1016/j.ssc.2012.04.072

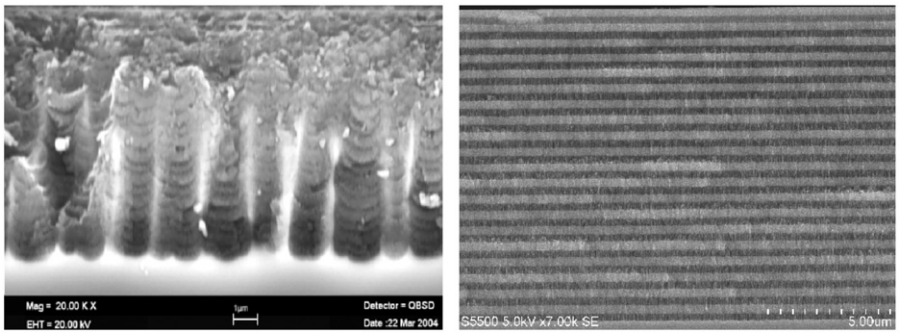

Fig. 1. SEM images of multilayer structures. On the left a high resistivity CSi:B sample (10 Ω cm), on the right a low resistivity CSi:B well formed photonic structure (1×10^{-3} Ω cm).

of electronic charge ($D(E)$) and densities of states (*DOS*) of **Si** clusters with **B** and **Al** impurities are reported, and in [16] using an *ab initio* code, the formation energies of co-doped (p and n type doping) nanocrystals were calculated. From first principles methods the segregation and ordering of the boron atoms in a Si(100) surface was studied [17]. They found a large relaxation of silicon atoms neighboring the **B** impurities. In Refs. [18,19] *ab initio* techniques were used to study the boron diffusion in silicon finding that if boron atoms are interstitial then a diffusion process occurs. Fritsch et al. [20,21] simulated a Si(001) surface with a half monolayer coverage of absorbed boron atoms reproducing experimental configuration results [22].

Here we simulate p-type silicon crystals with the highest number of silicon atoms in the unit cell used until now in a periodic solid configuration and by an *ab initio* code. In order to model experimental conditions we included the effect of temperature on some of their electronic properties. The concentration of boron atoms corresponds to the resistivity of the p-type silicon wafers used in the fabrication of *p−Si*. All these considerations result in a more realistic simulation model than previously reported.

The technical features of the *ab initio* software employed in our work, and the method used to generate the p-type silicon crystals (CSi:B) are described in the following section. In the results' section we present the structures of the CSi:B models, and their corresponding total and partial radial distribution functions (*RDFs*). We report the relative electronic densities *RelD*(*E*)*s* along planes which contain first **Si** neighbors of the **B** impurities. The *RelD*(*E*)*s* of two of the CSi:B models were calculated for a range of temperatures from 50 to 300 K to observe the reorganization of the electronic charge due to the thermal energy. Finally, in order to gather more electronic information about the CSi:B structures, we show their densities of states *DOS*.

2. Method

We generated 4 CSi:B models with 215, 214, 213, 212 **Si** atoms and 1, 2, 3 y 4 **B** atoms, respectively. The electronic structure was calculated using ABINIT that is an *ab initio* code based on total energy pseudopotential methods [23]. This code is based on the density functional theory (DFT) [24,25], and uses plane waves to expand the electronic wave functions. The ABINIT molecular dynamics routines are based on the Car-Parrinello scheme [26] and the temperature of these processes can be controlled by a variety of thermostats.

To construct and simulate the CSi:B models, we followed the next steps:

1. The diamond structure **Si** cell was replicated 3 times on each axis to obtain a crystalline supercell with 216 **Si** atoms, whose edges length is 16.29 Å and with density 2.33 g/cm^3.
2. To generate the CSi215B1 model, one **Si** atom was substituted by a boron atom; for the CSi214B2 another **Si** atom was replaced and so on for the two other models (CSi213B3 and CSi212B4). The boron atoms are near each other but they are not first neighbors as we are simulating a realistic heterogeneous distribution of impurities.
3. Once the CSi:B models have been constructed, an optimization of their geometries is implemented in the ABINIT code to obtain the lowest energy configuration. The VMD code was used to visualize the resulting optimized structures of the CSi:B models (Fig. 2(a)–(d)).
4. The *RDF* for all the models was calculated using the VMD code.
5. The **Si** atoms were simulated with a local type *Troullier-Martins* pseudopotential, and the **B** atoms with the *Troullier-Martins-Fermi*. The exchange and correlation energy functional used for the local density approximation (LDA) were the one proposed by Goedecker et al. [27].
6. For the geometry optimizations, a cutoff energy radius of 10 *Ha*, and tolerance force of 5×10^{-5} Ha/bohr were used. For the molecular dynamics jobs a Nos-Hoover thermostat and a time step of 2.41 fs were chosen.
7. To reproduce a high doping level of the experimental p-type silicon wafers, the CSi:B resistivity (ρ) was $\rho = 1 \times 10^{-3}$ Ω cm corresponding to a 1×10^{20} carriers/cm^3 concentration [28].

We are interested in emphasizing the changes on the electronic densities after including boron impurities in the silicon crystal. Then, we define a relative electronic density as:

$$RelD(E) = D(E)CSi : B - D(E)CSi, \quad (1)$$

where $D(E)CSi : B$ is the electronic density of a CSi:B model, and $D(E)CSi$ is the electronic density of a pure silicon crystal model. We obtained the $RelD(E)$ of each CSi:B model, on a plane determined by a **B** atom and two of its first **Si** neighbors. With this new variable we can observe directly how a boron atom influence its local environment. In order to visualize theses changes we considered $RelD(E) > 0.01$ electrons/Bohr^2.

To investigate the role of temperature on the electronic distribution around the boron atoms, the CSi215B1 and CSi212B4 models followed molecular dynamics (MD) processes on a range of 50–300 K. Once completed the MD implemented by the ABINIT code, we obtained their $D(E)$ and $RelD(E)$ with the method described above.

3. Results

The peaks' positions of all the total *RDF* in Fig. 3 indicate that CSi:B lattices are mostly crystalline. Their width reveals that the lattice disorder increases as the number of **B** atoms per simulation cell increases too. The partial *Si−B RDF* of Fig. 4 shows the

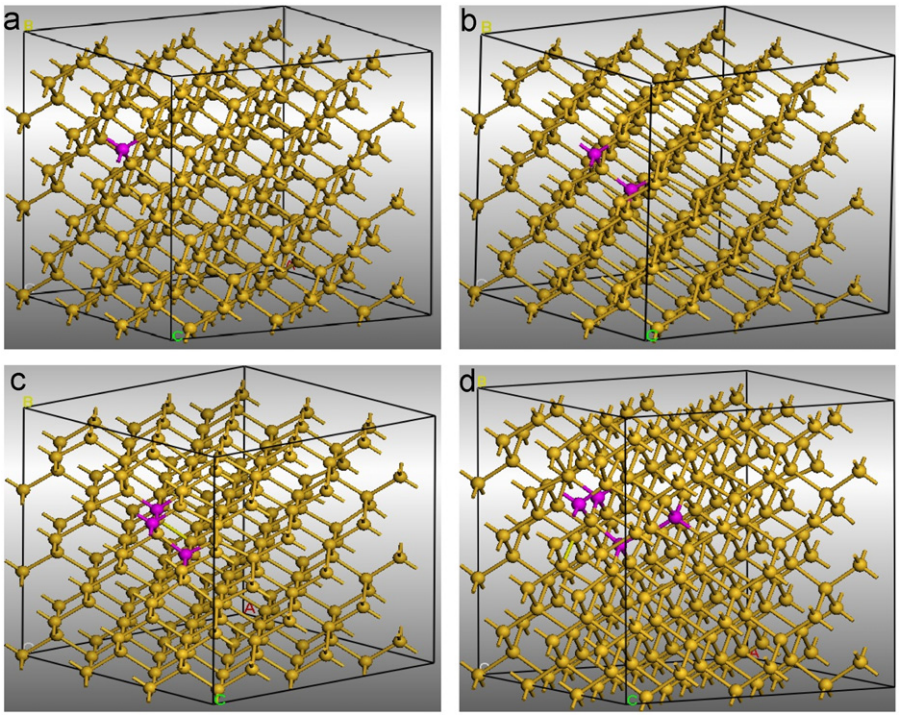

Fig. 2. (Color online) CSi:B models optimized structures: **Si** atoms in yellow and **B** atoms in magenta. (a) CSi215B1. (b) CSi214B2. (c) CSi213B3. (d) CSi212B4.

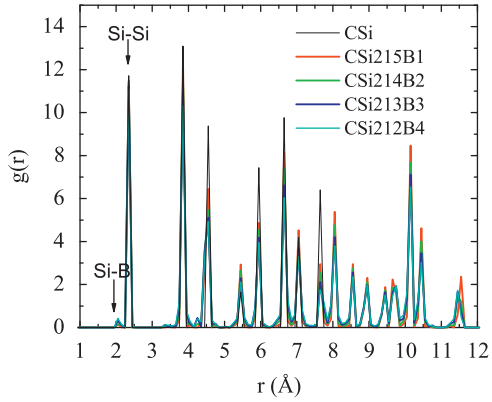

Fig. 3. (Color online) CSi:B total *RDF*. The pure **Si** crystal *RDF* (orange) shows the lattice long range order. The four total CSi:B *RDF* reveal the **B** impurities distortion.

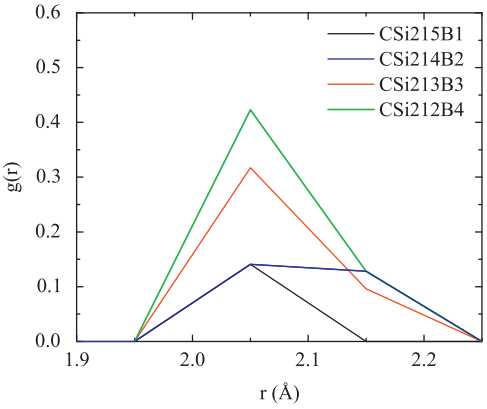

Fig. 5. (Color online) Total CSi:B *RDF* first peak corresponds to the probable bonding distance between the **Si** and **B** atoms. The Si–*B* bonding distance range from 1.95 to 2.25 Å, but the most probable occur at 2.05 Å.

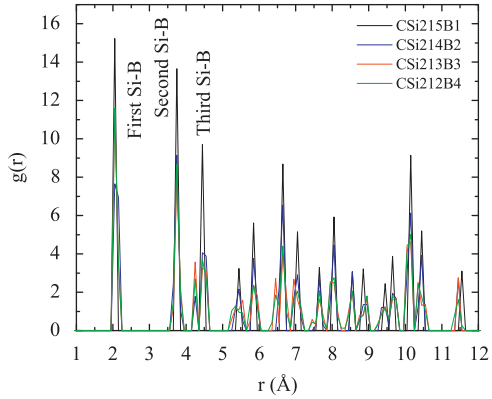

Fig. 4. (Color online) Partial Si–*B RDF* of the CSi:B models. For the models with 2, 3 and 4 **B** atoms the third neighbors are at 4.25 Å, and for the model CSi:B with just one **B** atom these neighbors are 20% away (4.45 Å). The **Si** atoms are attracted toward the closer **B** impurity.

disorder around the **B** silicon neighbors. The disorder around an impurity increases as well. The first total *RDF* peak (Fig. 5) suggests that **B** attracts the **Si** to the most probable Si–*B* bonding distance of 2.05 Å, which agrees with that reported in the literature [20–22].

The *D*(*E*) of the CSi:B models were calculated over different planes, we did not observe any influence of the boron atoms on the electronic densities farther than 3 Å from them. This observation was also made in [21]. We noticed that the planes containing one **B** atom and at least two of its first neighbors present the most important changes in the electronic charge distribution around the impurity. We concluded that if the number of **B** atoms per simulation cell increases, then the distortion of the **Si** network increases changing the *D*(*E*) appearance in the neighborhood of the **B** atom, as shown in Fig. 6(a)–(d). More impurities in the simulation cell cause a redistribution of the electronic density beyond the first silicon neighbors of the boron atoms, that is manifested by numerous hills surrounding the B atoms.

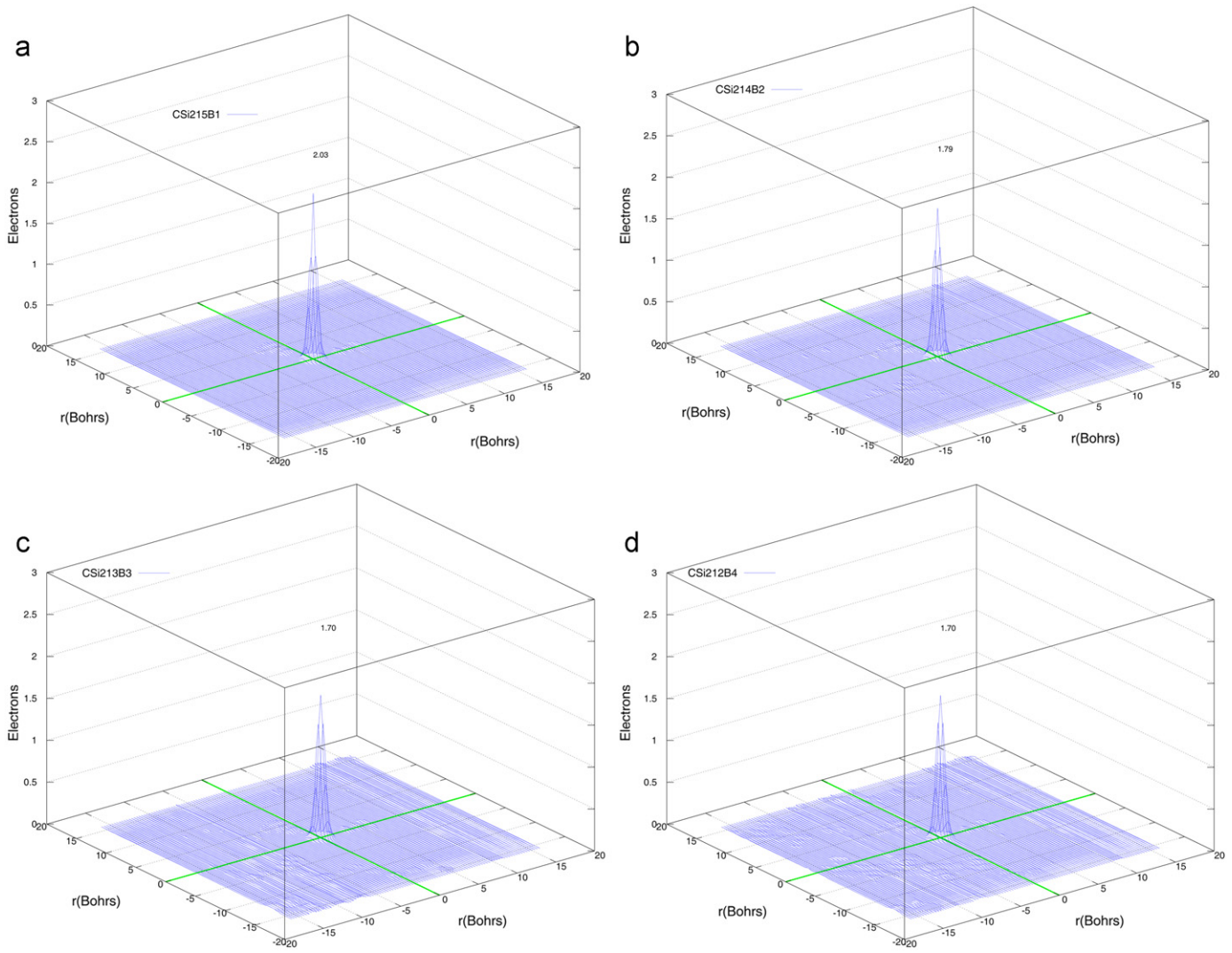

Fig. 6. (Color online) *RelD*(*E*) of the CSi:B models with (a) 1, (b) 2, (c) 3 and (d) 4 **B** atoms in the simulation cell. (a) CSi215B1. (b) CSi214B2. (c) CSi213B3. (d) CSi212B4.

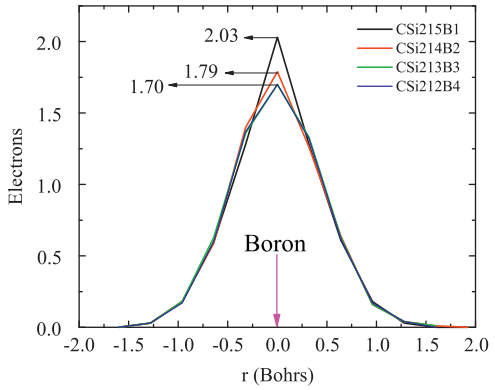

Fig. 7. (Color online) Relative electronic density profiles of the CSi:B models. As the number of boron impurities in the simulation cell increase, the electronic density is shortened.

The *RelD*(*E*) obtained were projected on a plane in order to compare their shape and size (see Fig. 7). We can notice that the relative electronic distributions are shortened as the number of impurities increases. We think that the electronic charge is shared by the necessary silicon atoms that are attracted by the boron atom. The width of the relative densities is on the range of 3.52–3.20 Bohrs, *i.e.* a radius of approximately 0.85 Å that coincides with the boron covalent radius.

Due to the fact that porous silicon is fabricated under room temperature conditions, we analyzed the role of temperature on the electronic charge distribution around the **B** atoms. We performed molecular dynamics (MD) of the CSi215B1 and CSi212B4 models at 0, 50, 150, 200, 250 and 300 K. After MD processes we obtained the corresponding *D*(*E*)*s* and *RelD*(*E*)*s*. We compared the size and shape of the CSi215B1 *RelD*(*E*)*s* and CSi212B4 *RelD*(*E*)*s*. No temperature dependence was observed. This is not surprising, considering that the CSi gap is $\sim$1.2 eV, and that 300 K is approximately 1/25 eV.

Finally, in Fig. 8(a)–(d) we present the *DOS* histograms of the CSi:B models where an appropriate energy interval was chosen. Their Fermi levels are at 0 eV. For comparison, in Fig. 9 we show the DOS histogram of a pure silicon crystal model. The values of the highest occupied molecular orbital (HOMO), lowest unoccupied molecular orbital (LUMO), impurity states and the gap (calculated as the difference LUMO-HOMO) are shown in Table 1. For the pure silicon crystal, the calculated band gap of 0.61 eV is less than the experimental value, an underestimation typical of the LDA calculations. The Fig. 8(a)–(d) show the impurity states in the CSi:B model gaps.

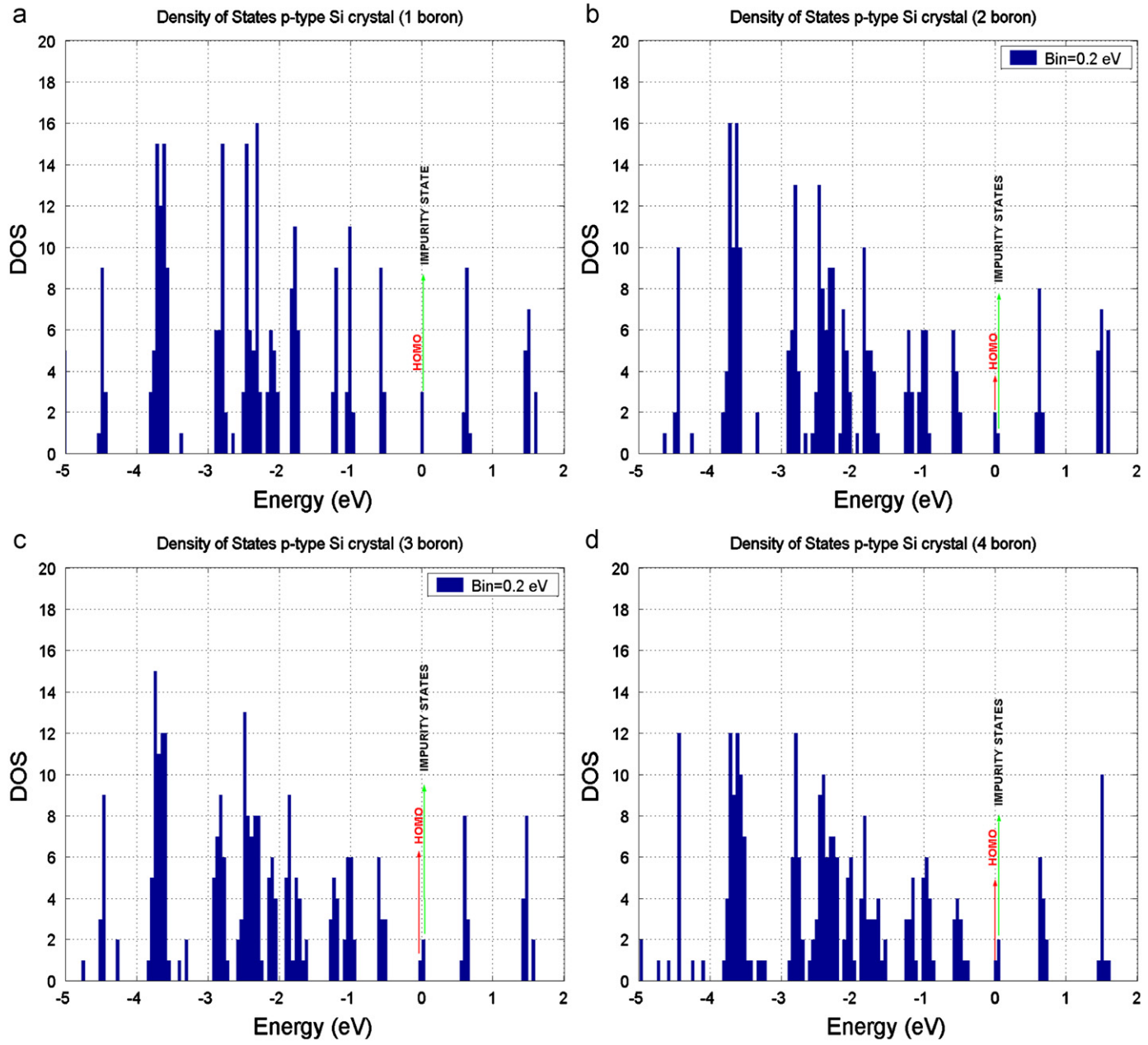

Fig. 8. (Color online) *DOS* histograms of the CSi:B models with (a) 1, (b) 2, (c) 3 and (d) 4 **B** atoms in the simulation cell. (a) CSi215B1. (b) CSi214B2. (c) CSi213B3. (d) CSi212B4.

4. Conclusions

It is well known that photonic structures made with porous silicon $p-$Si need to be fabricated using highly boron doped silicon wafers. This work is a first step to understand the role of boron impurities on the $p-$Si fabrication from an ab initio simulation perspective. Here we used four different models including boron atoms in crystalline silicon structures.

The *ab initio* simulation of the 4 CSi:B models reveals that the boron impurities modify the bonding length of their silicon neighbors to 2.05 Å approximately. The silicon atoms are attracted towards the boron and the CSi:B networks are distorted. On the other hand, the relative electronic densities of the CSi:B models are shortened as the number of impurities per simulation cell increase, and small hills appear in the plane where a boron atom lies. We conclude that these observations are the result of the electronic charge density balance with the necessary silicon atoms surrounding the impurities. We think that because the electronic density around the boron atom is large, the negative *HF* ion will avoid the boron atoms and its first silicon neighbors. Instead, it would attack the silicon atoms that are far from the boron impurity and as a consequence, determining the form of the porous silicon pores avoiding the boron atoms. The large negative charge distribution around the boron could explain the fact that these atoms are not removed from the porous silicon after an electrolytic erosion.

We are aware that the electrochemical attack to produce $p-$Si needs a current density to cave the pores on the silicon wafer in a finite time, and that current density could guide the *HF* attack, but we think that for very low current densities the number and the location of the boron impurities could control the *HF* trajectory attack. Because we did not find a change on the width of the $RelD(E)$ as a function of the temperature on the MD processes, we

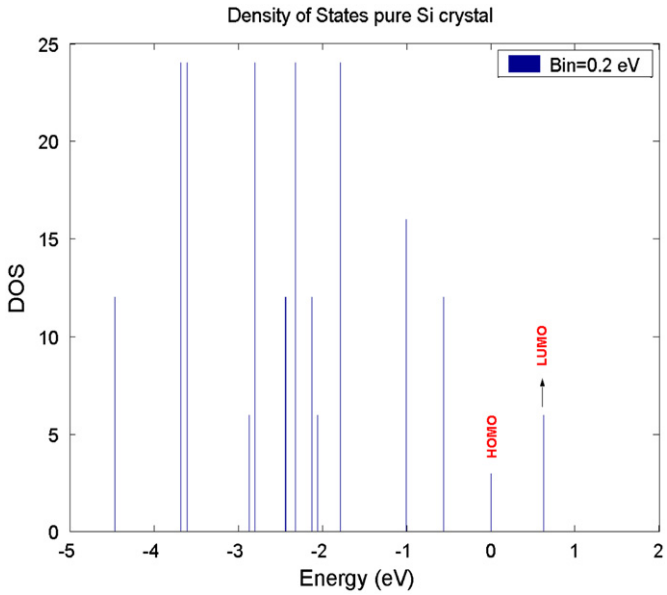

Fig. 9. *DOS* histogram of a pure silicon crystal model.

Table 1
Electronic parameters of the CSi:B models. We consider just the completely filled orbital case. All the energy values are reported on eV.

Model	HOMO	LUMO	B STATES	Gap
Si crystal	5.78	6.38	–	0.61
CSi215B1	5.76	6.36	5.76	0.61
CSi214B2	5.75	6.34	5.77	0.57
CSi213B3	5.75	6.32	5.75	0.57
CSi212B4	5.69	6.31	5.73	0.58

think that the most important factor to the $p-$Si morphology is the doping level of the crystalline silicon wafer.

Our goal is to understand the process of $p-$Si formation and how the morphology is related to the presence of boron atoms. We are currently working extending these calculations to porous silicon simulations.

Acknowledgements

The authors thank Dr. Yuri G. Rubo for helpful discussions, Héctor Daniel Cortés González for computer technical assistance and the M.C. José Campos for SEM images. Support from National University of México (UNAM) through a Postdoctoral Grant to E.R.L. Loustau is acknowledged. We thank the Computing and Information Technology Division of the UNAM and the National Supercomputing Center (CNS) for the computer resources. This work was supported in part by DGAPA-UNAM under grant PAPIIT IN106510.

References

[1] L.T. Canham, Appl. Phys. Lett. 57 (1990) 1046–1048.
[2] A.G. Cullis, L.T. Canham, P.D.J. Calcott, Appl. Phys. Rev. 82 (1997) 909–965.
[3] M. Ohmukai, M. Taniguchi, Y. Tsutsumi, Mater. Sci. Eng. B. 86 (2001) 26–28.
[4] G. Polisski, D. Kovalev, G. Dollinger, T. Sulima, F. Koch, Physica B. 273–274 (1999) 951–954.
[5] J.E. Lugo, J.A. del Río, J. Tagüe na-Martínez, J. Appl. Phys. 81 (1997) 1923–1928.
[6] J. Tagüe na-Martínez, .Rubo Yuri G, M. Cruz, M.R. Beltrán, C. Wang, Appl. Surf. Sci. 142 (1998) 564–568.
[7] M. Cruz, R. Beltrán, C. Wang, J. Tagüe na-Martínez, Y.G. Rubo, Phys. Rev. B. 59 (1999) 15381–15387.
[8] V. Agarwal, J. A del Rio, G. Malpuech, M. Zamfirescu, A. Kavokin, D. Coquillat, D. Scalbert, M. Vladimirova, B. Gil, Phys Rev. Lett. 92 (2004) 097401–097406.
[9] V. Agarwal, J.A. del Rio, Int. J. Mod. Phys. B. 20 (2006) 99–110.
[10] A.G. Palestino, M.B. de la Mora, J.A. del Río, C. Gergely, E. Pérez, Appl. Phys. Lett. 91 (2007) 1219091–1219093.
[11] R. Nava, J. Phys. D: Appl. Phys. 43 (2010) 455102–455107.
[12] M. B de la Mora, O.A. Jaramillo, R. Nava, J. Tagüe na-Martínez, J.A. del Río, Sol. Energy Mater. Sol. Cells. 93 (2009) 1218–1224.
[13] J. Tagüe na-Martínez, J.A. del Río, Y.G. Rubo, R. Nava, Segunda Reunión Mexicana sobre Física Matemática y Física Experimental, in: F.J. Uribe, L.S. García-Colín, E. Díaz-Herrera (Eds.), Statistical Physics and Beyond, vol. 757, American Institute of Physics, 2005. ISBN 0-7354-0242-6.
[14] V. Lehmann, H. Föll, J. Electrochem. Soc. 137 (1990) 653–659.
[15] J.A. Cogordan, L.E. Sansores, A.A. Valladares, J. Non-Crys. Solids. 181 (1995) 135–145.
[16] F. Iori, S. Ossicini, Physica E. 41 (2009) 939–946.
[17] M. Ramamoorthy, E.L. Briggs, J. Bernholc, Phys. Rev. B. 59 (1999) 4813–4820.
[18] W. Windl, M.M. Bunea, R. Stumpf, S.T. Dunham, M.P. Masquelier, Phys. Rev. Lett. 8321 (1999) 4345–4348.
[19] M. Hakala, M.J. Puska, R.M. Nieminen, Phys. Rev. B. 61 (1999) 8155–8161.
[20] J. Fritsch, J.B. Page, K.E. Schmidt, G.B. Adams, Phys. Rev. B. 57 (1998) 9745–9756.
[21] J. Chang, M.J. Stott, Phys. Rev. B. 53 (1996) 13700–13704.
[22] Y. Wang, R.J. Hammers, E. Kaxias, Phys. Rev. Lett. 74 (1995) 403–406.
[23] M.C. Payne, M.P. Teter, D.C. Allan, T.A. Arias, J.D. Joannopoulos, Rev. Mod. Phys. 64 (1992) 1045–1096.
[24] P. Hohenberg, W. Kohn, Phys. Rev. B. 136 (1964) 864–871.
[25] W. Kohn, L.J. Sham, Phys. Rev. A. 140 (1965) 1133–1138.
[26] R. Car, M. Parrinello, Phys. Rev. Lett. 55 (1985) 2471–2474.
[27] S. Goedecker, M. Teter, J. Huetter, Phys. Rev. B. 54 (1996) 1703–1710.
[28] W.R. Thurber, R.L. Mattis, Y.M. Liu, J. Filliben, J. Electrochem. Soc.: Solid State Science and Technology 127 (1980) 2291–2294.